Structure Tuning of Crown Ether Grafted Conjugated Polymers as the Electron Transport Layer in Bulk-Heterojunction Polymer Solar Cells for High Performance

*Yi-Lun Li, Yu-Shan Cheng, Po-Nan Yeh, Sih-Hao Liao, and Show-An Chen**

A series of novel electron transport (ET) polymers composed of different conjugated main chains (fluorene, thiophene, and 2,7-carbazole) and crown ether side chain (crown ether, aza-crown ether and amine) is presented for bulk-heterojunction polymer solar cells with poly(3-hexylthiophene) (P3HT) or poly[[4,8-bis[(2-ethylhexyl)oxy]benzo [1,2-b:4,5-b′] dithiophene-2,6-diyl] [3-fluoro-2-[(2-ethylhexyl)carbonyl]thieno[3,4-b]thiophenediyl]](PTB7) as the active polymer and aluminum metal as the cathode. Unexpectedly, it is found that the main chain of ET polymers has a greater effect on the interfacial dipole than the side chain, even when attaching a high polarity group. The electron-rich bridge atom of the main chain may also contribute appreciably to the interfacial dipole. When used as the ET layer, all of these polymers can generate an optical interference effect for redistribution of the optical electric field as an optical spacer and, therefore, allow more light to be absorbed by the active layer, thus leading to an increase in short-circuit current density. They can also block hole diffusion to the cathode and prevent electron–hole recombination during the ET process. Among the five ET polymers investigated, PCCn6 is the most effective one, providing a remarkable improvement in the power conversion efficiency (measured in air) of the device to 8.13% compared to 5.20% for PTB7:[6,6]-phenyl-C_{71}-butyric acid methyl ester ($PC_{71}BM$).

1. Introduction

Bulk-heterojunction (BHJ) polymer solar cells[1] (PSCs) with an active layer composed of a conjugated polymer as the donor and a fullerene derivative as the acceptor have attracted great attention because of their ease of fabrication, promising flexibility, and capability for large-scale and low-cost production. Poly(3-hexylthiophene) (P3HT) with its high regioregularity and [6,6]-phenyl-C_{61}-butyric acid methyl ester ($PC_{61}BM$) are the most representative conjugated polymer donor material and acceptor material, respectively. The power conversion efficiencies (PCEs) for PSCs based on these two materials can reach 4 to 5%.[2] To enhance the PCE by design of the active layer, one can design an acceptor with a higher lowest unoccupied molecular orbital (LUMO) level to increase the open-circuit voltage (V_{OC}); this results in PCBM-like molecules[3–5] and C_{60} bisadducts.[6–9] Another way is to replace P3HT with lower-bandgap polymers, thus allowing promotion of the PCE from 5 to over 7%,[10–14] as reported for the donors such as poly[[4,8-bis[(2-ethylhexyl)oxy]benzo[1,2-b:4,5-b′] dithiophene-2,6-diyl][3-fluoro-2-[(2-ethylhexyl)carbonyl] thieno[3,4-b]thiophenediyl]] (PTB7) along with the fullerene derivative acceptor [6,6]-phenyl-C_{71}-butyric acid methyl ester ($PC_{71}BM$).[12]

In addition to material design of the active layer, the insertion of an electron transport layer (ETL) between the active layer and metallic cathode can also increase the PCE, the ETL can be alkali metal complexes (e.g., LiF,[15] CsF,[16] Cs_2CO_3),[17,18] metal oxides (e.g., TiO_2,[19] ZnO),[20–22] self-assembled monolayers (SAMs),[23–26] or alcohol/water-soluble polymesr.[27–32] In order not to dissolve the hydrophobic active layers, the polymer ETL must be hydrophilic. Additionally, the main chain of the polymer ETL must be conjugated, otherwise the low conductivity will cause poor device performance. In 2011, Bazan and co-workers[28] proposed an alcohol soluble copolymer of thiophene and fluorene derivative as the ETL in PSCs with the active layer PCDTBT:$PC_{71}BM$. This copolymer provides an interfacial dipole to the cathode, which can enhance the built-in electrical field of the device and further improve the PCE from 5.3% to 6.5%. In the same year, Cao and co-workers[29] proposed another alcohol (with minor amount of acid) soluble fluorene derivative, poly[(9,9-bis(3′-(*N*,*N*-dimethylamino)propyl)-2,7-fluorene)-*alt*-2,7-(9,9–dioctylfluorene)] (PFN) as the ETL for PSCs with PTB7: $PC_{71}BM$, resulting in a great increase in the PCE from 5.00% to 8.37% due to the promoted built-in electrical field from the interfacial dipole induced by PFN. The importance of the interfacial dipole in the performance of organic and polymer electronics has been reviewed extensively in the literature.[33,34]

In 2013, we proposed[32] an alcohol-soluble, fluorene-based conjugate polymer with crown ether attached to the side chain as the ETL for PSCs with P3HT:ICBA, resulting in an increase

Y.-L. Li, Y.-S. Cheng, P.-N. Yeh, S.-H. Liao, Prof. S.-A. Chen
Chemical Engineering Department and Frontier Research Center on Fundamental and Applied Sciences of Matters
National Tsing-Hua University
Hsinchu 30013, Taiwan, ROC
E-mail: sachen@che.nthu.edu.tw

DOI: 10.1002/adfm.201401428

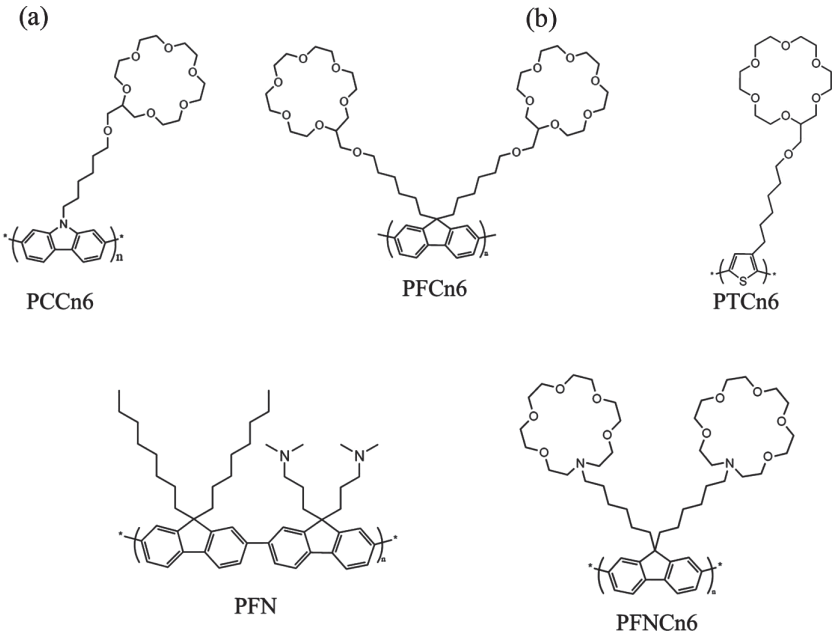

Scheme 1. Structures of polymers with different main chains and side chains as the ETL.

in the PCE from 3.87% to 6.35% (Al as the cathode) or 5.78% to 6.77% (Ca/Al as the cathode). Moreover, chelating the crown ether in PFCn6 with potassium cation (PFCn6:K^+) resulted in promoted electron collection and thus further enhanced the short-circuit current density, J_{SC}, from 10.43 to 11.65 mA cm^{-2}. PCE was also improved from 5.78% to 7.5% when Ca/Al was used as the cathode.

Here, we synthesize a series of conjugated polymers with different main chains and crown ether side chains (PTCn6, PFCn6, PCCn6, PFN, and PFNCn6; see **Scheme 1** for the chemical structures) to explore the effects of polymer structure on interfacial dipole strength and optical spacing effect. We find that the main chain of the conjugated polymer, rather than side chain, mainly determines the interfacial dipole strength meaning that the molecular design of the main chain is much more important for promotion of the interfacial dipole and, therefore, V_{OC}. We simulate the device with various ETLs and find that the ETL is capable of rearranging the optical electric field distribution established by combining the incident light and reflected light from the mirror cathode and therefore enhancing the absorption of the active layer except when the absorption spectra overlaps with that of the active layer, such as PTCn6. In addition, the polymer ETL can also lower the current leakage. Consequently, by introducing such an ETL, the PCE of the PSC is enhanced. Specifically, by introducing PCCn6 as the ETL, the PCE is improved from 5.20% to 8.13% in the PTB7: $PC_{71}BM$ system and from 3.02% to 3.91% in the P3HT: $PC_{61}BM$ system.

2. Result and Discussion

2.1. Interfacial Dipole

We synthesized five alcohol soluble conjugated polymers with different main chain and side chain as ETL and their chemical structures and energy levels are as shown in Scheme 1 and Supporting Information Table S1, respectively. In the BHJ PSCs, V_{OC} has been correlated with the energy level difference between the highest occupied molecular orbital (HOMO) of the electron donor and LUMO of the electron acceptor.[35] In addition, V_{OC} was also found to be influenced by the difference between the work functions of the two electrodes.[36] Consequently, introducing an ETL, that induces the interfacial dipole (Δ), which is taken to be the difference between the energy level of the metal cathode with ETL and the work function of the cathode, can result in an increase in the work function of the cathode (closer to the vacuum level)[27,32] and therefore a larger difference of the work functions between two electrodes, resulting in a higher V_{OC}.[36]

Results from ultraviolet photoelectron spectroscopy (UPS) measurements, which show the Δ between different ETLs and the aluminium electrode, are shown in **Figure 1** and their sequence is as follow: PCCn6 (0.73 eV) > PFNCn6 (0.66 eV) > PFN (0.64 eV) > PFCn6 (0.60 eV) > PTCn6 (0.30 eV). The 2,7-carbazole main chain results in larger Δ than fluorene and thiophene main chains, under same side chain structure, which are as follow: PCCn6 (0.73 eV) > PFCn6 (0.60 eV) > PTCn6 (0.30 eV). The higher V_{oc} of the PCCn6 compared to the PFCn6 may also be caused by the higher polarity bridged atom (nitrogen in PCCn6) based on the similar repeat unit structures. On the other hand, we found that a higher polarity group on side chain results in larger Δ for the same main chain, fluorene, as manifested by the sequence PFNCn6 (0.66 eV) > PFN (0.64 eV) > PFCn6 (0.60 eV). However, the Δ between PCCn6 and PFCn6 is 0.13 eV larger than that between PFNCn6 and PFCn6 (0.06 eV), indicating that the structure of the main chain has greater influence on Δ than the structure of the side chain does, even though a higher polarity group, such as an amine group, is attached. As mentioned above, larger Δ causes larger V_{OC} applied to solar cell device. P3HT:$PC_{61}BM$ and PTB7:$PC_{71}BM$ systems are as shown in **Table 1**. PCCn6 has the largest Δ in our synthesized ETLs, hence it possesses the largest V_{OC}: 0.634 V in the P3HT:$PC_{61}BM$ system and 0.732 V in the PTB7:$PC_{71}BM$ system.

As discussed above, we found that introducing conjugated polymer as the ETL could increase the vacuum level of the metallic cathode due to forming Δ at the interface between the ETL and the cathode. Therefore, larger Δ corresponds to higher rise vacuum level of the metal and results in a larger work function difference between the two electrodes, which leads to an enhancement of V_{OC}. Consequently, the structure of the main chain has a greater influence on V_{OC} than the side chain does.

2.2. Optical Interference

In the solar cell, the sun light travels through the ITO anode to enter into the active layer, then the photocurrent is generated due to a dissociation of exciton formed by absorption of light

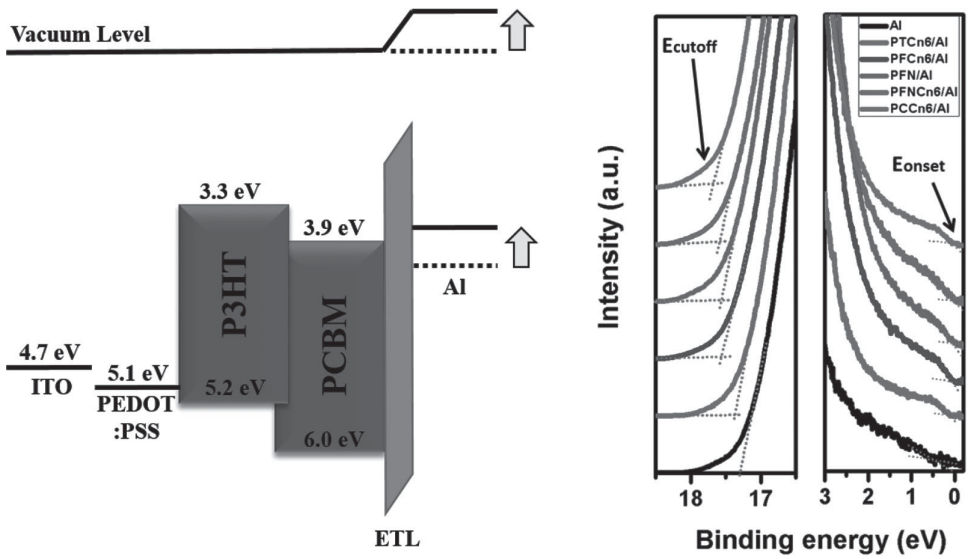

Figure 1. a) Energy diagram of the solar cell device with ETLs. b) The UPS spectra of different ETLs deposited on Al.

by the active layer. The remaining unabsorbed light travels to the metallic mirror cathode and then reflects back to the active layer and is reabsorbed. If the absorption ranges of the ETL and active layer overlap or partially overlap, the ETL will absorb some reflected light from the cathode, which can be utilized by the active layer. Therefore, a suitable ETL material should not absorb the same wavelength range of light as the active layer to avoid possible loss of sun light. However, the absorption of PTCn6 is located in the visible region, which overlaps with the absorption of most active polymers. Thus, PTCn6 is not suitable as an ETL. If the ETL does not absorb the light, which is able to be utilized by the active layer, and meanwhile enhances the absorption of the active layer, this ETL then can further enhance light absorption of the active layer by redistributing the optical electric field. Some metal oxides, such as ZnO[20] and TiO_2,[19] have been reported to meet the purpose by allowing the active layer to absorb more light and therefore improve the J_{SC} of the solar cell. Here, we used an ellipsometer to measure the refractive indices (n) and extinction coefficients (k) of four ETLs and three active layers (Supporting Information Figure S1) and we simulated the optical electric field distribution using the ESSENTIAL MACLEOD software package (Thin Film Center, Inc., Tucson, USA).

Table 1. Interfacial dipole between different ETL and an aluminum electrode and the V_{OC} of the devices with different ETLs for P3HT:PC_{61}BM under pre-annealing processing and in the PTB7:PC_{71}BM system.

Electrode	Energy level (from UPS)[a)]	Interfacial dipole [Δ]	V_{OC}[b)] [V]	V_{OC}[c)] [V]
Al	–4.28 eV	–	0.461	0.653
PTCn6/Al	–3.98 eV	0.30 eV	0.494	0.713
PFCn6/Al	–3.68 eV	0.60 eV	0.564	0.726
PFN/Al	–3.64 eV	0.64 eV	0.572	0.724
PFNCn6/Al	–3.62 eV	0.66 eV	0.607	0.727
PCCn6/Al	–3.55 eV	0.73 eV	0.634	0.732
Ca/Al[d)]	–	–	0.613	0.726

[a)]UPS data are calculated from the UPS spectrum (Figure 1b); [b)]The V_{OC} from devices with structure: ITO/PEDOT:PSS(25 nm)/P3HT:PC_{61}BM(1:0.8)(60 nm)/annealing 130 °C,10 min/ETL(10 nm)/Al(100 nm); [c)]The V_{OC} from devices with structure: ITO/PEDOT:PSS(25 nm)/PTB7:PC_{71}BM(1:1.5)(70 nm)/ETL(10 nm)/Al(100 nm); [d)]Since the calcium is too active to measure the precise energy level.

Following the first report on polymer optical spacers that enhance light absorption of the active polymer,[32] we studied the structure properties of ETLs by simulating the optical electrical field distribution in the device. The simulated optical electric field distributions of the device structure: indium tin oxide (ITO; 150 nm)/poly(3,4-ethylenedioxythiophene):polystyrene sulfonate (PEDOT:PSS; 25 nm)/P3HT:PC_{61}BM(1:0.8)(60 nm)/ETL(10 nm)/Al(100 nm) are shown in **Figure 2**. For the device without an ETL (Figure 2a), the strongest peaks of the optical electric fields are not all located inside the active layer for the three wavelengths of incident light, 400 nm, 500 nm, and 600 nm, which lie in the absorption range of the active polymer. However, after incorporation of 10 nm ETL (PCCn6, PFNCn6, PFCn6 or PFN), all the strongest optical electric field spectra move toward the interior of the active layer region making the light harvesting of the active layer more effective (Figure 2b–e). The same phenomenon is also observed for the other active layer systems, P3HT:ICBA and PTB7:PC_{71}BM (Supporting Information Figure S2 and Figure S3, respectively). These simulation results indicate that the main chain and side chain structures of these ETL polymers cause little difference in the optical electric field distribution when comparing the same thickness. We further investigated the thickness effect of the ETL on the optical electric field adjustment, specifically for PCCn6 with the three active layer systems. The results of simulations for thicknesses from 0 to 25 nm at 477 nm incident light wavelength (which is the absorption maximum of P3HT as shown in Supporting Information Figure S1d) indicates that as the thickness of PCCn6 increases to 25 nm, the optical electric field peak is located at the center, as shown in Figure 2f for the P3HT:PC_{61}BM system. In addition, the same result also appears

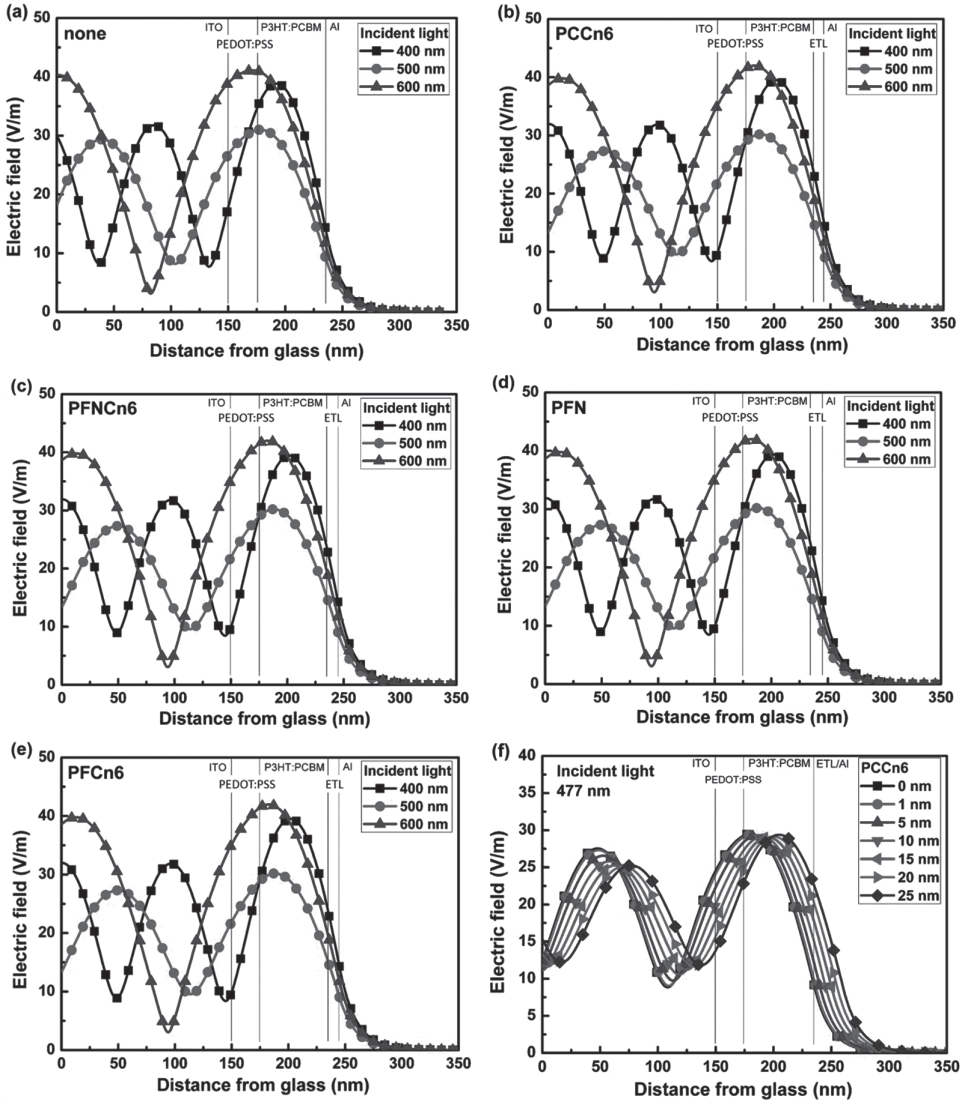

Figure 2. Simulated optical electric field of solar cell device with the device structure: ITO (150 nm)/PEDOT:PSS (25 nm)/P3HT:$PC_{61}BM$ (60 nm)/ETL/Al (100 nm): a) without ETL and with 10 nm b) PCCn6, c) PFNCn6, d) PFN, and e) PFCn6 under the incident light of 400 nm, 500 nm, and 600 nm. f) Different PCCn6 thickness under the incident light at 477 nm (the absorption maximum of P3HT).

for P3HT:ICBA and PTB7:$PC_{71}BM$ systems. However, thicker PCCn6 also slightly weakens the optical electric field strength and lowers the J_{SC} of the device. Thus, the trade-off relation between good optical electric field maximum location and strong light intensity caused by ETL thickness variation implies a presence of optimal ETL thickness for the best device performance.

In order to further explore effects on absorption enhancement of active layer caused by inserting the ETL, we simulate the reflected spectrum of the devices with different ETL and calculate the change in absorption, $\Delta\alpha$. The formula used for the calculation is as follow:[19]

$$\Delta\alpha(\lambda) \approx -\frac{1}{2d}\ln\left(\frac{I'_{out}(\lambda)}{I_{out}(\lambda)}\right) \quad (1)$$

where λ is wavelength, d is thickness of active layer, $I'_{out}(\lambda)$ is the intensity of the reflected light from the device with or without ETL, and $I_{out}(\lambda)$ is the intensity of reflected light from the reference device (glass/Al). To lower the light loss and avoid complication arising from the conducting layers, we simulate the device in the absence of ITO and PEDOT:PSS, and prepare the device glass/active layer/ETL/Al.[19] After the insertion of the ETLs, PCCn6, PFNCn6, PFN and PFNCn6, the absorption peak of P3HT:$PC_{61}BM$ locating at around 477 nm from the simulated absorption spectra is significantly enhanced in similar extent for these ETLs as shown in **Figure 3**a. The differences of $\Delta\alpha$ at the maximum absorption peak of active layer among these ETL are insignificant in three active systems, P3HT:$PC_{61}BM$, P3HT:ICBA (as shown in Supporting Information Figure S4a) and PTB7:$PC_{71}BM$ (as shown in Figure S4c), respectively.

As mentioned above the thickness of the ETL plays an important role on optical electric field distribution, therefore, we further investigate the effect of thickness on $\Delta\alpha$ for PCCn6 with

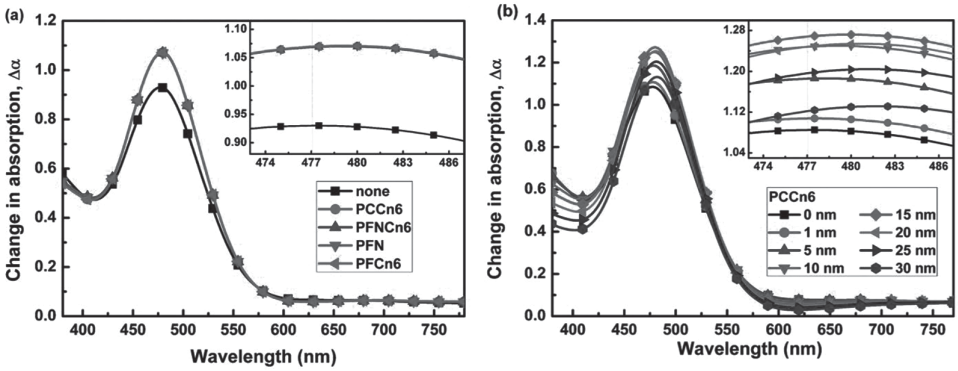

Figure 3. Change in absorption with a) the same thickness of different ETLs and b) the different thickness of PCCn6. The simulated device structure is glass/P3HT:$PC_{61}BM$ (60 nm)/ETL/Al (100 nm). The insets in (a,b) are the amplification of the absorption near the $\Delta\alpha$ maximum.

P3HT:$PC_{61}BM$. The simulated $\Delta\alpha$ at 477 nm shows a maximum at the PCCn6 thickness 15 nm (as shown in Figure 3b), indicating that using an optimal thickness of PCCn6 is necessary to gain the largest $\Delta\alpha$ for maximum absorption in the active layer, as shown in Supporting Information Table S2. The best performance and the highest J_{SC} of 8.59 mA cm^{-2} is reached with a PCCn6 thickness of 9.2 nm (thickness calculation is the same as in ref. [29]), which is not in correspondence with the simulation results of 15 nm reported above. We presume that the polymer ETL is semiconducting, rather than conducting, and the thinner ETL has to be taken to compensate for its lower charge transport properties. However, the simulation cannot take these points into consideration, which is why the optimal thickness in the device is thinner than that from simulations.

Consequently, the present polymer ETL also has the capability of optical electric field adjustment for increasing the absorbance of the active layer. However, the main chain and side chain structures of these ETL polymers bring little difference in adjusting the optical electric field distribution with the same thickness. As long as the ET material does not absorb the same range wavelength of light as active layer, which avoids possible loss of sun light, it can redistribute the optical electric field, resulting in more light absorption in the active layer with an appropriate thickness of the ETL.

2.3. Device Performance

The annealing process was found to improve the crystallinity of P3HT in P3HT:PCBM system, which can result in higher J_{SC}.[2] There are two types of annealing used in this work for the P3HT:PCBM system: one is the pre-annealing (annealing after spin-cast active layer and before thermal deposition of the metal cathode) and the other is the post-annealing (annealing after thermal deposition of the metal cathode). The latter type can provide higher device performance. The performance of the devices with different ETLs under post-annealing are listed in **Table 2**. Because the metal cathode film quality can also be affected by the post-annealing process, the effect of the interfacial dipole would be less obvious, and therefore small changes in V_{OC} are observed. The performance of the device with PFN is not reported in Table 2 because it is extremely poor. During the device fabrication, a small amount of acetate acid is needed to enhance the solubility of PFN in common organic solvent. We presume that in the post-annealing process, the acetate acid may diffuse to the active layer and quench the excitons, leading to poor performance with a PCE of 1.83%.

Additionally, our ETLs are capable of adjusting the optical field distribution and can therefore provide the strongest optical electric field located within an active layer in addition to enhancing the absorbance of the active layer. Compared to the devices without ETLs, the device shows largely enhancement on J_{SC} with the insertion of PCCn6 (8.66 mA cm^{-2}), PFNCn6 (8.11 mA cm^{-2}), PFCn6 (7.93 mA cm^{-2}) and without ETL (7.45 mA cm^{-2}) in the P3HT:$PC_{61}BM$ system. In particular, the J_{SC} of the device with PTCn6 (7.34 mAc m^{-2}) is lower than that without an ETL (7.45 mA cm^{-2}), which is due to the absorption spectrum of PTCn6 and P3HT overlapping and causing a weakening of the reflected light from the metallic

Table 2. Device performance of different ETL under post-annealing process (150 °C,10 min) in P3HT:$PC_{61}BM$ system with device structure: ITO/PEDOT:PSS(25 nm)/P3HT:$PC_{61}BM$(1:0.8)(60 nm)/ETL(10 nm)/Al(100 nm).

ETL	V_{OC} [V]	J_{SC} [mA cm^{-2}]	FF [%]	PCE [%]	R_{sh}[a)] [Ω cm^2]	R_s [Ω cm^2]
none	0.640	7.45	63.3	3.02	1261	1.73
PTCn6	0.650	7.34	61.5	2.94	1446	1.96
PFCn6	0.650	7.93	67.9	3.50	1381	0.58
PFNCn6	0.652	8.11	67.0	3.54	1399	0.82
PCCn6	0.655	8.66	69.0	3.91	1770	0.52
PFCn6:K^+	0.650	7.75	60.2	3.03	–	–

[a)]The R_{sh} and R_s calculations are the same as in ref. [37].

Table 3. Device performance of different ETL in PTB7:$PC_{71}BM$ system with device structure: ITO/PEDOT:PSS(25 nm)/PTB7:$PC_{71}BM$ (1:1.5)(70 nm)/ETL(10 nm)/Al(100 nm).

ETL	V_{OC} [V]	J_{SC} [mA cm^{-2}]	FF [%]	PCE [%]	R_{sh} [Ω cm^2]	R_s [Ω cm^2]
none	0.653	12.65	62.9	5.20	640	3.98
MeOH	0.687	13.57	67.7	6.31	742	1.16
PTCn6	0.713	13.20	66.6	6.28	859	1.49
PFCn6	0.726	14.12	69.1	7.07	917	1.21
PFN	0.724	15.01	70.0	7.61	925	1.19
PFNCn6	0.727	14.86	74.1	8.03	1195	0.48
PCCn6	0.732	15.19	73.2	8.13	1152	0.46
PFCn6:K^+	0.740	11.87	70.4	6.18	–	–

cathode to the active layer. However, the J_{SC} of the device with PTCn6 (13.20 mA cm^{-2}) is larger than that without ETL (12.65 mA cm^{-2}) in PTB7:$PC_{71}BM$ system, which is due to the methanol effect on the active layer causing a higher J_{SC}.[28] Similarly, the absorption spectra of PTCn6 and PTB7 overlap with each other in certain wavelength ranges, which leads to a lower J_{SC} of the device. On the other hand, in PTB7:$PC_{71}BM$ device the J_{SC} with insertion of ETLs are larger than that without ETL similar to those in P3HT:$PC_{61}BM$ system. Independent of the type of active system, the different ETL has only a small influence on active layer $\Delta\alpha$ under same thickness as shown in Figure 3a.

The enhancement of J_{SC} shows obvious differences among these ETLs. This is because the ETL could also affect the shunt resistance (R_{sh}) and series resistance (R_s) of the device and therefore is also responsible for the enhancement of J_{SC}, as listed in **Table 3**. The device with PCCn6 possesses largest R_{sh} (1770 Ω cm^2 and 1152 Ω cm^2 in the P3HT:$PC_{61}BM$ system and the PTB7:$PC_{71}BM$ system, respectively), which corresponds to a small leakage current as reflected in the smallest R_s (0.52 Ω cm^2 and 0.46 Ω cm^2 in P3HT:$PC_{61}BM$ system and in PTB7:$PC_{71}BM$ system, respectively).

Furthermore, the electron transport was promoted as the crown ether side chain chelated potassium cation (K^+), which resulted in higher performance in the P3HT:ICBA device.[32] The PCE of P3HT:ICBA device is lower than in our previous report, as shown in Supporting Information Table S3, because the P3HT and ICBA, purchased from Rieke Metals Inc., are not from the same production batch. In P3HT:$PC_{61}BM$ and PTB7:$PC_{71}BM$ systems, however, the PCE of the devices were not enhanced. An explanation for why interaction of K^+ does not work for P3HT:$PC_{61}BM$ and PTB7:$PC_{71}BM$ systems will be given in our future work.

In general, PCCn6 has a stronger interfacial dipole, which results in a larger V_{OC} and optical electric field adjustment capability. Moreover, PCCn6 can effectively lower the leakage current and improve the electron collection in the device. Including all the advantages above, the PCCn6 device shows a PCE improvement from 3.02% to 3.91% for P3HT:$PC_{61}BM$ system, and from 5.20% to 8.13% for the PTB7:$PC_{71}BM$ system (the current density–voltage (*I*–*V*) curve is shown in **Figure 4**).

3. Conclusions

In the design of alcohol-soluble conjugated polymers for use as ETLs in PSCs with hydrophobic active layers for PCE promotion, the conjugated aromatic main chain with the electron-rich bridge nitrogen atom is preferred. It able to introduce higher interfacial dipoles for higher V_{oc} and to enhance absorption of the active layer through its capability for rearranging optical electric field within the device (expect for those with absorption spectra that overlap with the light absorption of the polymer in the active layer). In addition, its HOMO level should be deeper than the light-absorbing polymer in the active layer for blocking holes. Among the ETLs investigated, PCCn6 is the

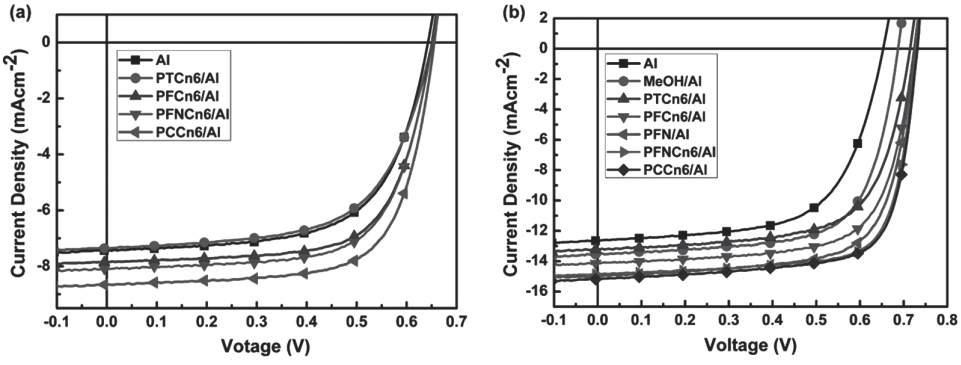

Figure 4. *I*–*V* curve of the device with different ETLs for a) P3HT:$PC_{61}BM$ and b) PTB7:$PC_{71}BM$ system.

best and provides a PCE improvement from 3.02% to 3.91% for the P3HT:PC_{61}BM system and from 5.20% to 8.13% for the PTB7:PC_{71}BM system.

Supporting Information

Supporting Information is available from the Wiley Online Library or from the author.

Acknowledgements

The authors thank the Ministry of Education and the National Science Council for financial support through Project NSC-101–2120-M-007–004, NSC-102–2633-M-007–002 and NSC-102–222-E-007–131.

Received: May 2, 2014
Revised: June 14, 2014
Published online: September 1, 2014

[1] G. Yu, J. Gao, J. C. Hummelen, F. Wudl, A. J. Heeger, *Science* **1995**, *270*, 1789.
[2] W. Ma, C. Yang, X. Gong, K. Lee, A. J. Heeger, *Adv. Funct. Mater.* **2005**, *15*, 1617.
[3] G. Zhao, Y. He, Z. Xu, J. Hou, M. Zhang, J. Min, H.-Y. Chen, M. Ye, Z. Hong, Y. Yang, Y. Li, *Adv. Funct. Mater.* **2010**, *20*, 1480.
[4] J. A. Mikroyannidis, A. N. Kabanaks, S. S. Sharma, G. D. Sharma, *Adv. Funct. Mater.* **2011**, *21*, 746.
[5] Y. He, B. Peng, G. Zhao, Y. Zou, Y. Li, *J. Phys. Chem. C* **2011**, *115*, 4340.
[6] Y. He, H.-Y. Chen, J. Hou, Y. Li, *J. Am. Chem. Soc.* **2010**, *132*, 1377.
[7] G. Zhao, Y. He, Y. Li, *Adv. Mater.* **2010**, *22*, 4355.
[8] X. Meng, W. Zhang, Z. Tan, Y. Li, Y. Ma, T. Wang, L. Jiang, C. Shu, C. Wang, *Adv. Funct. Mater.* **2012**, *22*, 2187.
[9] X. Fan, C. Cui, G. Fang, J. Wang, S. Li, F. Cheng, H. Long, Y. Li, *Adv. Funct. Mater.* **2012**, *22*, 585.
[10] Y. Liang, Y. Wu, D. Feng, S.-T. Tsai, H.-J. Son, G. Li, L. Yu, *J. Am. Chem. Soc.* **2009**, *131*, 56.
[11] H.-Y. Chen, J. Hou, S. Zhang, Y. Liang, G. Yang, Y. Yang, L. Yu, Y. Wu, G. Li, *Nat. Photonics* **2009**, *3*, 649.
[12] Y. Liang, Z. Xu, J. Xia, S.-T. Tsai, Y. Wu, G. Li, C. Ray, L. Yu, *Adv. Mater.* **2010**, *22*, E135.
[13] A. Najari, S. Beaupré, P. Berrouard, Y. Zou, J.-R. Pouliot, C. Lepage-Pérusse, M. Leclerc, *Adv. Funct. Mater.* **2011**, *21*, 718.
[14] J. Yuan, Z. Zhai, H. Dong, J. Li, Z. Jiang, Y. Li, W. Ma, *Adv. Funct. Mater.* **2013**, *23*, 885.
[15] C. J. Brabec, S. E. Shaheen, C. Winder, N. S. Sariiftci, P. Denk, *Appl. Phys. Lett.* **2002**, *80*, 1288.
[16] X. Jiang, H. Xu, L. Yang, M. Shi, M. Wang, H. Chen, *Sol. Energy Mater. Sol. Cells* **2009**, *93*, 650.
[17] F.-C. Chen, J.-L. Wu, S. S. Yang, K.-H. Hsieh, W.-C. Chen, *J. Appl. Phys.* **2008**, *103*, 103721.
[18] H.-H. Liao, L.-M. Chen, Z. Xu, G. Li, Y. Yang, *Appl. Phys. Lett.* **2008**, *92*, 173303.
[19] J. Y. Kim, S. H. Kim, H.-H. Lee, K. Lee, W. Ma, X. Gong, A. J. Heeger, *Adv. Mater.* **2006**, *18*, 572.
[20] Z. Liang, Q. Zhang, O. Wiranwetchayan, J. Xi, Z. Yang, K. Park, C. Li, G. Cao, *Adv. Funct. Mater.* **2012**, *22*, 2194.
[21] Y. Sun, J. H. Seo, C. J. Takacs, J. Seifter, A. J. Heeger, *Adv. Mater.* **2011**, *23*, 1679.
[22] H. Cheun, C. Fuents-Hernandez, J. Shim, Y. Fang, Y. Cai, H. Li, A. K. Sigdel, J. Meyer, J. Maibach, A. Dindar, Y. Zhou, J. J. Berry, J.-L. Bredas, A. Kahn, K. H. Sandhage, B. Kippelen, *Adv. Funct. Mater.* **2012**, *22*, 1531.
[23] H.-L. Yip, S. K. Hau, N. S. Baek, H. Ma, A. K.-Y. Jen, *Adv. Mater.* **2008**, *20*, 2376.
[24] H. Ma, H.-L. Yip, F. Huang, A. K.-Y. Jen, *Adv. Funct. Mater.* **2010**, *20*, 1371.
[25] X. Bulliard, S.-G. Ihm, S. Yun, Y. Kim, D. Choi, J.-Y. Choi, M. Kim, M. Sim, J.-H. Park, W. Choi, K. Cho, *Adv. Funct. Mater.* **2010**, *20*, 4381.
[26] S. Lacher, Y. Matsuo, E. Nakamura, *J. Am. Chem. Soc.* **2011**, *133*, 16997.
[27] S.-H. Oh, S.-I. Na, J. Jo, B. Lim, D. Vak, D.-Y. Kim, *Adv. Funct. Mater.* **2010**, *20*, 1977.
[28] J. H. Seo, A. Gutacker, Y. Sun, H. Wu, F. Huang, Y. Cao, U. Scherf, A. J. Heeger, G. C. Bazan, *J. Am. Chem. Soc.* **2011**, *133*, 8416.
[29] Z. He, C. Zhong, X. Huang, W.-Y. Wong, H. Wu, L. Chen, S. Su, Y. Cao, *Adv. Mater.* **2011**, *23*, 4636.
[30] C. He, C. Zhong, H. Wu, R. Yang, W. Yang, F. Huang, G. C. Bazan, Y. Cao, *J. Mater. Chem.* **2010**, *20*, 2617.
[31] K. Yao, L. Chen, Y. Chen, F. Li, P. Wang, *J. Mater. Chem.* **2011**, *21*, 13780.
[32] S.-H. Liao, Y.-L. Li, T.-Z. Jen, Y.-S. Cheng, S.-A. Chen, *J. Am. Chem. Soc.* **2012**, *134*, 14271.
[33] S. Braun, W. R. Salaneck, M. Fahlman, *Adv. Mater.* **2009**, *21*, 1450.
[34] H. Ishii, K. Sugiyama, E. Ito, K. Seki, *Adv. Mater.* **1999**, *11*, 605.
[35] M. C. Scharber, D. Mühlbacher, M. Koppe, P. Denk, C. Waldauf, A. J. Heeger, C. J. Brabec, *Adv. Mater.* **2006**, *18*, 789.
[36] V. D. Mihailetchi, L. J. A. Koster, P. W. M. Blom, *Appl. Phys. Lett.* **2004**, *85*, 970.
[37] W.-J. Ke, G.-H. Lin, C.-P. Hsu, C.-M. Chen, Y.-S. Cheng, T.-H. Jen, S.-A. Chen, *J. Mater. Chem.* **2011**, *21*, 13483.